Available online at www.sciencedirect.com

ScienceDirect

Procedia Structural Integrity 41 (2022) 646–655

Structural Integrity Procedia

www.elsevier.com/locate/procedia

2nd Mediterranean Conference on Fracture and Structural Integrity

# On The Fracture Toughness Of PPS And PPA Reinforced With Glass Fiber

Alexandru Isaincu[a,*], Dan Micota[b], Liviu Marşavina[b]

[a]Politehnica University of Timişoara, Department of Steel Structures and Structural Mechanics, Ioan Curea, No. 1, Timişoara 300223, Romania
[b]Politehnica University of Timişoara, Department of Mechanics and Strength of Materials, Victoria Square, No. 2, Timişoara 300222, Romania

**Abstract**

The presented article discusses the fracture behavior of two short fiber reinforced polymers (SFRP): a polyphthalamide (PPA) with glass fiber inclusions of 33% (GF33) and a polyphenylene sulfide (PPS) with glass fiber inclusions of 40% (GF40). The behavior of these two materials was characterized as brittle and highly orthotropic in accordance with the tensile strength tests in Micota, Isaincu, and Marşavina 2021. The influence of the fiber orientation on the fracture toughness and crack propagation path is assessed by means of physical testing and numerical simulations. Mode I and mode II fracture toughness were determined on edge crack triangular (ECT) specimens Aliha, Hosseinpour, and Ayatollahi 2013 subjected to three-point bending. Symmetrical loading was applied for mode I fracture toughness and asymmetrical loading for mode II. Three fiber orientations of 0°, 45° and 90° were considered. The numerical simulations were performed using CASCA and FRANC2D.


Peer-review under responsibility of the MedFract2Guest Editors.

*Keywords:* Fracture toughness; polyphthalamide; polyphenylene sulfide; three point bending; FRANC2D.

## 1. Introduction

The current global context points towards pushing the automotive market to ask for more performance at lower cost and less weight from its products. These harsh requirements are transferred to materials manufacturing of automotive products. High performance engineering polymers with glass fiber reinforcement, similar to the ones approached in

* Corresponding author. Tel.: +40-720-537-935.
*E-mail address:* alexandru.isaincu@student.upt.ro

2452-3216 
Peer-review under responsibility of the MedFract2Guest Editors.
10.1016/j.prostr.2022.05.073

this paper, are being used more often in the automotive industry. These materials can be seen in chassis and suspension load bearing applications as well as traditional powertrain component applications. The understanding of how these types of materials work is essential for an efficient part design.

**Nomenclature**

| | |
|---|---|
| SFRP | short fiber reinforced polymers |
| PPA | polyphthalamide |
| GF33 | 33% glass fiber inclusions |
| PPS | polyphenylene sulfide |
| GF40 | 40% glass fiber inclusions |
| ECT | edge crack triangular |
| t | thickness of the specimen |
| b | notch/crack width |
| a | notch/crack length |
| h | height of the specimen |
| w | top width of the specimen |
| W | bottom width of the specimen |
| P | load |
| SIF | stress intensity factor of a crack |
| $K_I$ | mode I stress intensity factor |
| $K_{II}$ | mode II stress intensity factor |
| $Y_I$ | geometric factor for mode I |
| $Y_{II}$ | geometric factor for mode II |
| $E_1$ | Young's modulus corresponding to 0° fiber orientation |
| $E_2$ | Young's modulus corresponding to 90° fiber orientation |
| $\nu_{12}$ | Poisson's ratio |
| $G_{12}$ | shear modulus |
| $K_{Ic}$ | mode I fracture toughness |
| $K_{IIc}$ | mode II fracture toughness |
| $f_u$ | tensile strength |
| SEM | scanning electron microscope |

The aim of this work is to investigate the influence of fiber orientation on the fracture toughness of PPA GF33 and PPS GF40 materials determined on ECT specimens. In the past, several research studies were conducted to assess the effects of fiber orientation on different mechanical properties in Köbler et al. 2018, Bernasconi et al. 2007, Holmström, Hopperstad, and Clausen 2020, Jørgensen, Andreassen, and Salaberger 2019 and many others.

The ECT specimen was used to determine the fracture toughness of polymethyl methacrylate (PMMA) by Aliha, Bahmani, and Akhondi 2016 and rock material in Aliha, Hosseinpour, and Ayatollahi 2013. What the previous mentioned papers have in common is that the investigated material is isotropic. Small number of studies are made for orthotropic materials, especially on PPA. For the PPS, some values for fracture toughness can be found in Tanaka, Kitano, and Egami 2014, Friedrich 1985 and Karger-Kocsis and Friedrich 1987. For other orthotropic materials, fracture toughness values were given in Karger-Kocsis and Friedrich 1988 and Torabi et al. 2021.

In this paper, the fracture toughness of PPA GF33 and PPS GF40 is studied by means of physical testing and numerical simulations.

## 2. Experimental details

### *2.1. Materials*

The two investigated materials are PPA GF33 and PPS GF40. Both materials are provided by the Solvay Group. In the market, these materials can be found under the trade name of Amodel AE-4133, respectively Ryton R-4-270.

The 33% weight fraction glass fiber reinforced polyphthalamide (PPA GF33), approached in this paper, represents a high-performance polymer with abundant utilization in the automotive industry. This material is part of the thermoplastic branch of polymers and has a semi-crystalline structure. Some of the incentives to use such a material are the very good mechanical properties, good dimensional stability, elevated work temperature ranges and good processing characteristics. The Amodel AE-4133 grade features a high heat deflection temperature, high flexural modulus, high tensile strength, as well as excellent creep resistance and low moisture absorption.

The other material described in this paper is a polyphenylene sulfide reinforced with glass fiber 40% weight fraction (PPS GF40). It is also a high performance semi-crystalline structured thermoplastic, with excellent mechanical properties, high temperature resistance and low water absorption. These properties make it very useful in automotive powertrain applications such as coolant pumps and other thermal management components, engine components, etc. In terms of processing, PPS is more delicate than PPA, due to its low melt viscosity, higher precision molding tools are required, but if processed correctly, outstanding dimensional stabilities can be reached. The Ryton R-4-270 is described as a compound that provides enhanced mechanical strength after constant or repeated exposure to high temperature water.

In terms of cost to performance ratio, these types of materials bridge the gap between high volume, moderate performance engineering polymers and low volume, high-cost specialty thermoplastics.

The principal mechanical properties of the mentioned materials were tested and presented in Micota, Isaincu, and Marşavina 2021. From there, it can clearly be seen that, the fiber orientation has an important effect on the mechanical properties.

### *2.2. Sample preparation*

The ECT specimens were obtained from larger square plates. The nominal dimensions of the plates are 100 mm length, 100 mm width and thickness (t) of 3.175 mm (1/8 of an inch). These plates were obtained using injection molding process and were delivered directly by the supplier (Solvay Group). The injection molding process is performed in such a way that leads to a good and uniform fiber orientation in the middle of the plate. All specimens were obtained using water jet cutting technologies. The cutting dimensions of the plates, for all three considered orientations, are presented in Fig. 1.

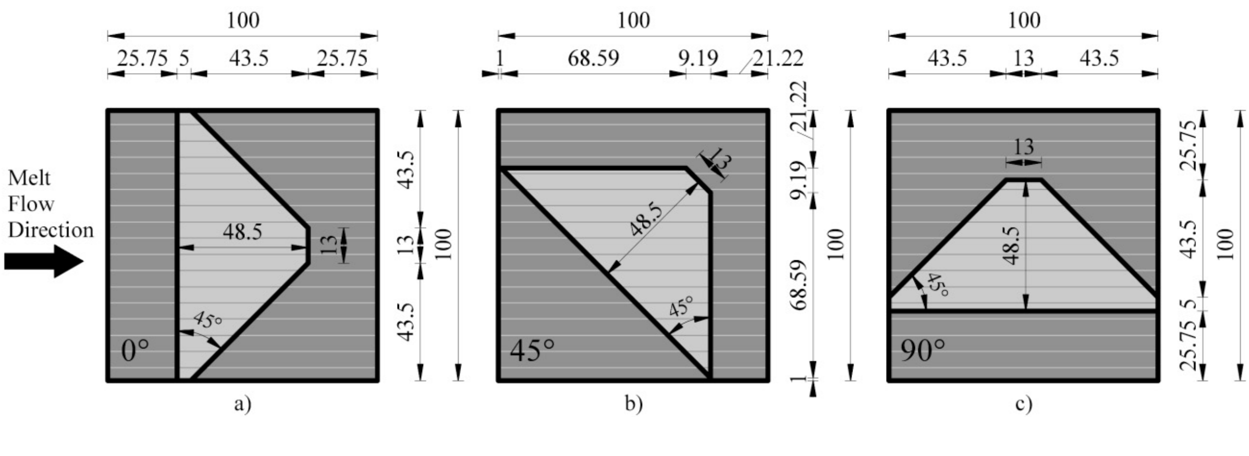


Fig. 1. Specimen cutting from the original square plate considering an orientation angle of (a) 0°, (b) 45° and (c) 90° compared with the melt flow direction.

To avoid to not have a pointy surface in the location where the force will be applied, the triangle was transformed into a trapeze. This transition will allow a more uniform application of the force and will avoid the local crushing of the material.

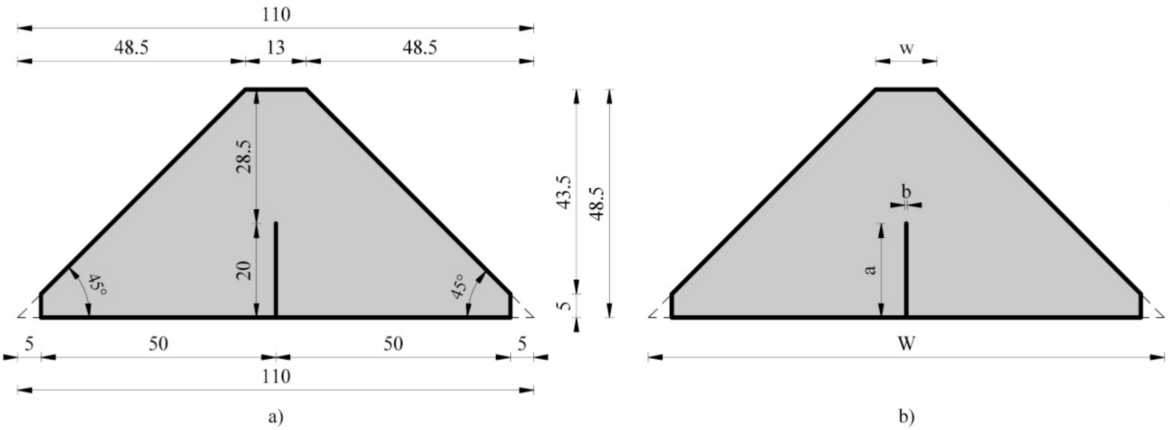


Fig. 2. Nominal dimensions of the (ECT) specimen (a) and the main geometric parameters (b).

All the nominal dimensions of the ETC specimen are presented in Fig. 2. To prepare the samples for testing, a thin fret saw was used to cut a notch in the middle of the bottom side of the trapeze. The width of the notch/crack (b) is around 0.55 mm. This cut was created perpendicular to the bottom edge. The nominal length of the notch/crack (a) is 20 mm. The specimen height (h) is 48.5 mm. The top width (w) and the bottom width (W) were kept at 13 mm and 100 mm respectively. For the 45° orientation samples, the nominal bottom width is 110 mm, instead of 100 mm, due to how the specimens were extracted from the plates.

*2.3. Three-point bending tests*

To investigate the toughness of the two materials, a series of three-point bending tests were performed on the ECT specimens. These tests were conducted under mode I (crack opening) and mode II (crack sliding) loading conditions.

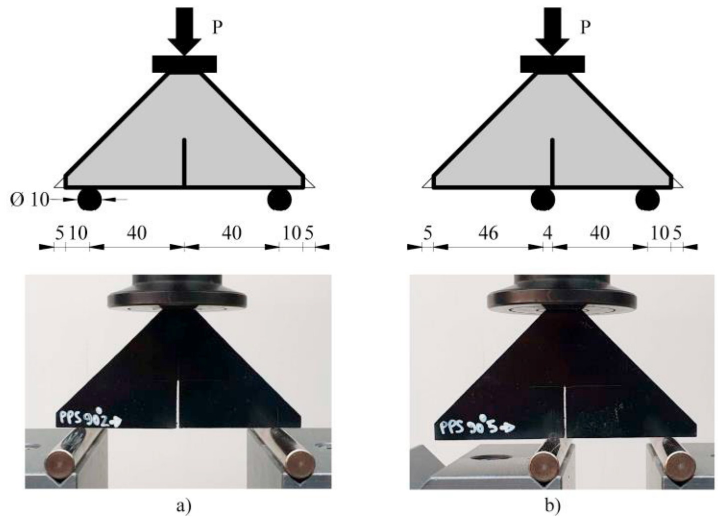


Fig. 3. Schematic representations (at the top) and real-life pictures (at the bottom) of the test setup considering (a) symmetrical loading for mode I and (b) asymmetrical loading for mode II.

A schematic representation of the test setup can be seen in Fig. 3. A total number of 66 specimens (33 for PPA and 33 for PPS) were produced and tested. Sets of 5 up to 6 specimens were considered for each loading type and fiber orientation.

All tests were conducted at room temperature, in normal humidity conditions. A vertical compressive force (P) was applied up to the fracture load using a Zwick Roell Z005 universal testing machine. The speed of the testing equipment was set to 5 mm/min.

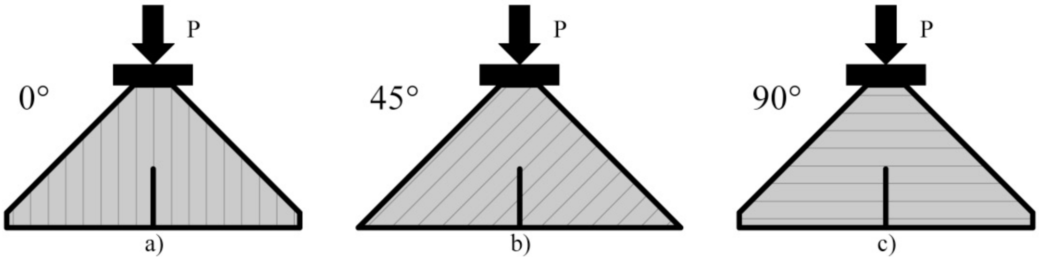


Fig. 4. Orientation angle of (a) 0°, (b) 45° and (c) 90° between fiber orientation and crack orientation.

Fig. 4 depicts the relationship between fiber orientation and crack orientation. If the orientation of the fibers coincides with the orientation of the crack, the orientation angle was defined as 0°. If the orientation of the fibers is perpendicular to the orientation of the crack, the orientation was defined as 90°. For our case, the orientation angle is similar with the fiber orientation angle.

In conclusion, two materials (PPA GF33 and PPS GF40), under two loading conditions (Fig. 3) and three orientations (Fig. 4) were tested.

## 3. ECT specimen calibration

The Stress Intensity Factors (SIF's) solutions in mode I ($K_I$) and mode II ($K_{II}$) are defined as follows:

$$K_I = Y_I \frac{P\sqrt{\pi a}}{2ht} \tag{1}$$

$$K_{II} = Y_{II} \frac{P\sqrt{\pi a}}{2ht}. \tag{2}$$

where: $Y_I$ and $Y_{II}$ are the geometrical factors for mode I, respectively mode II, P is the load, a is the crack length, h is the height and t is the thickness of the ECT specimen. The analytical solution is available only for SIF's and not for the geometrical factors.

Table 1. Orthotropic properties.

| Material | $E_1$ [MPa] | $E_2$ [MPa] | $\nu_{12}$ [MPa] | $G_{12}$ [MPa] |
|---|---|---|---|---|
| PPA GF33 | 11698 | 5616 | 0.370 | 2414 |
| PPS GF40 | 15923 | 7385 | 0.410 | 3167 |

The non-dimensional SIF's solutions were determined by means of numerical investigation using FRANC2D software. FRANC2D is a free two-dimensional fracture analysis software, developed at Cornell University in New York State. It was funded by the U.S. National Science Foundation, NASA, the U.S. Navy and other agencies. The software has multiple functions such as: modeling stress / fracture analysis, stress intensity factor calculator, crack propagation / growth and fatigue crack growth analysis. The software integrates two individual parts: a simple mesh generator, called CASCA, and the solver / post-processor, called FRANC2D.

The simulations were performed considering an orthotropic material with the properties provided in Tab. 1. The numerical models are shown in Fig. 5 for both symmetric and asymmetric loading.

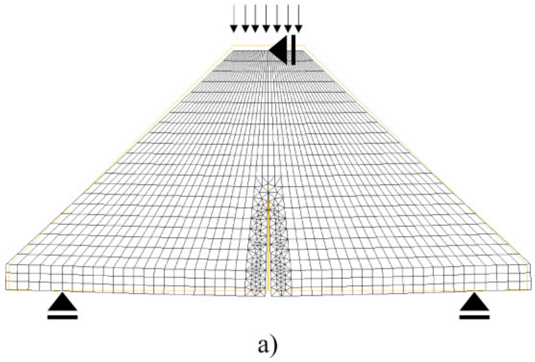


Fig. 5. ECT specimen deformation in FRANC2D under (a) symmetrical loading conditions and (b) asymmetrical loading conditions.

A total number of 1820 eight-nodded plane stress elements connected in 3749 nodes were used for each model. Singular elements were considered around the crack to model the square root singularity at the crack tip. The orientation of the orthotropic material was changed in steps of 15°, between 0° and 90°. The SIF's values were obtained using the displacement extrapolation technique. In all cases, a constant force of 1000 N was applied at the top part of the specimen.

The variation of $Y_I$ and $Y_{II}$ with fiber orientation angle is shown in Fig. 6, for PPA material, side by side with the values corresponding to homogeneous material (red dotted lines). A linear isotropic material model, with $E_I$ as Young's Modulus (corresponding to 0° fiber orientation), was used in FRANC2D to generate that value.

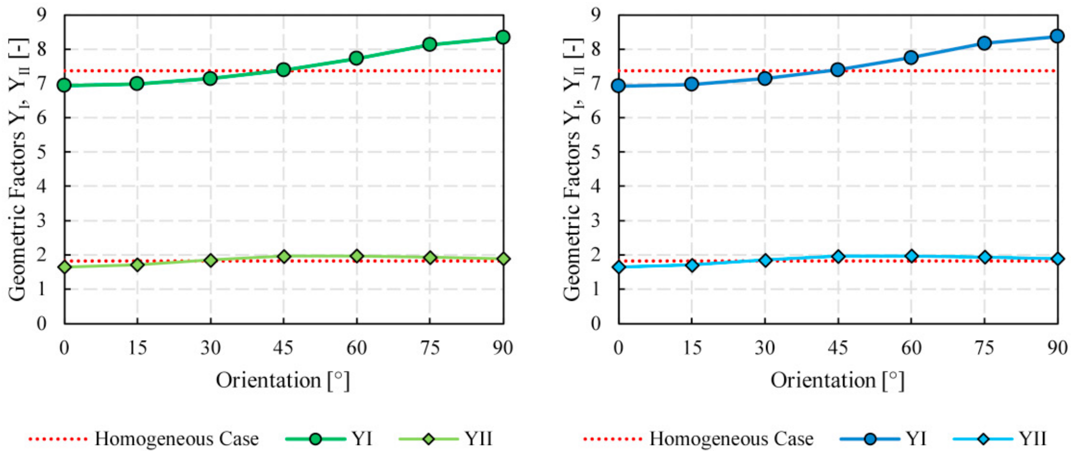


Fig. 6. Variation of non-dimensional SIF's with the orientation angle for PPA GF33 (left) and PPS GF40 (right).

Comparing the two materials, insignificantly small variation in terms of geometrical factors can be distinguished for both $Y_I$ and $Y_{II}$. An increasing trend can be seen for $Y_I$ with the increase in the fiber orientation. For $Y_{II}$, up to 45°, there is an increasing trend. This tendency changes between 45° and 90°.

For both materials, the $Y_I$ orthotropic solution at 45° overlaps with the homogeneous solution. Because the variation of $Y_{II}$ is minimal, at all angles, the orthotropic solution is close to the homogeneous one.

## 4. Results and discussions

Typical force-displacement curves obtained during testing are presented in Fig. 7, for all modes, orientations and both materials. The force-displacement curves show a linear elastic behavior up to maximum load and a brittle fracture. The initial rigidity of the specimens is similar for a certain considered mode (ex: for PPS GF33, Mode I, the force-displacement curves are clustered together). The rigidity decreases for mode I loading conditions, compared to mode II. It can clearly be seen that mode II loading conditions led to higher forces and displacements, in comparison with mode I. Mode II presents, overall, higher displacements and forces, in comparison with mode I. A small indentation was observed at the adjacent support to the specimen axis for asymmetric loading.

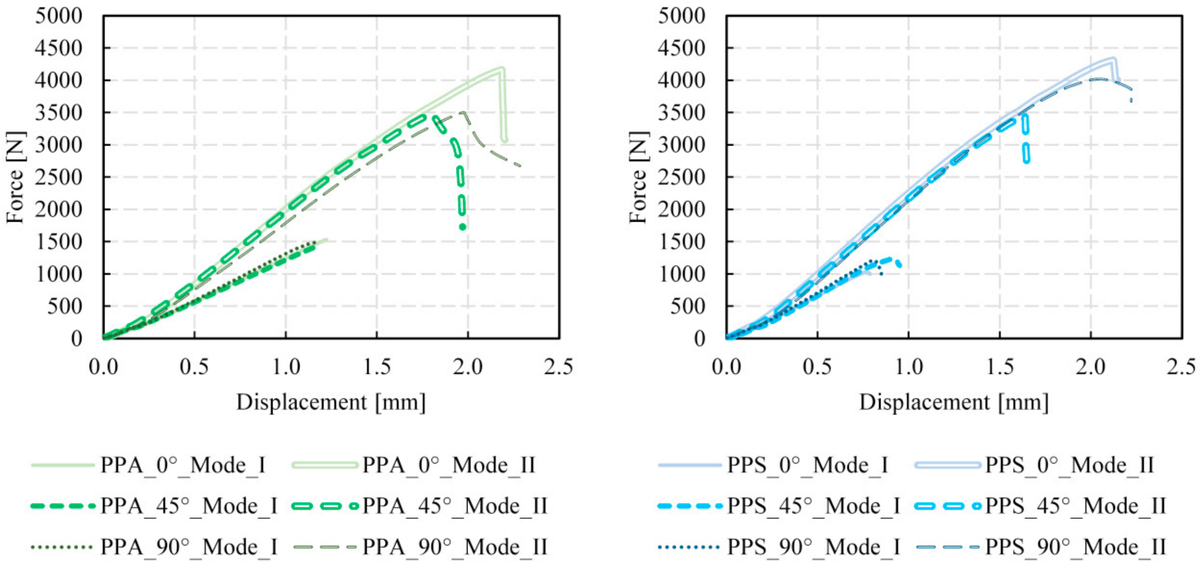


Fig. 7. Typical force-displacement curves for PPA GF33 (left) and PPS GF40 (right) function of orientation angle and tested mode.

An overview of all breaking forces (as a mean value), standard deviations and coefficients of variation are presented in Tab. 2.

Table 2. Test results in terms of breaking force, standard deviation and coefficient of variation.

| Material | Mode | Orientation Angle [°] | Breaking force [N] | Standard deviation [N] | Coefficient of variation [%] |
|---|---|---|---|---|---|
| PPA | I | 0 | 1187 | 255 | 22% |
| | | 45 | 1288 | 134 | 10% |
| | | 90 | 1428 | 77 | 5% |
| | II | 0 | 4162 | 309 | 7% |
| | | 45 | 3342 | 242 | 7% |
| | | 90 | 3158 | 363 | 11% |
| PPS | I | 0 | 1000 | 37 | 4% |
| | | 45 | 1208 | 61 | 5% |
| | | 90 | 1182 | 34 | 3% |
| | II | 0 | 4377 | 112 | 3% |
| | | 45 | 3327 | 193 | 6% |
| | | 90 | 3474 | 460 | 13% |

Based on these tests, the maximum load was considered for calculation of the fracture toughness in mode I ($K_{Ic}$) and mode II ($K_{IIc}$), using eq. (1) and (2). The variation of fracture toughness $K_{Ic}$ and $K_{IIc}$ with fiber orientation angle is shown in Fig. 8.

The fracture toughness in mode I increases with the orientation angle. A decreasing tendency can be seen in mode II. For both materials, the trends are similar.

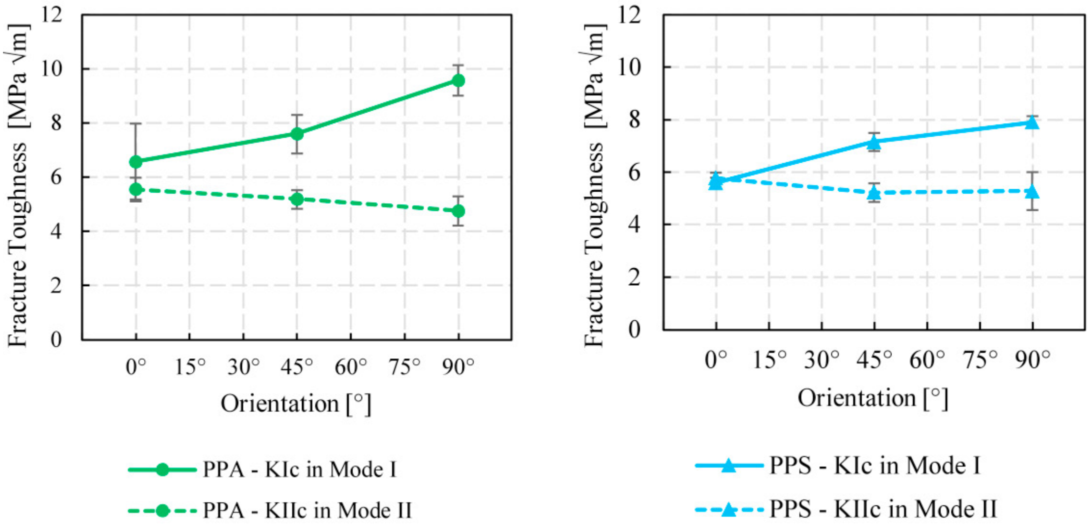


Fig. 8. Fracture toughness $K_{Ic}$ and $K_{IIc}$ for PPA GF33 (left) and PPS GF40 (right).

Closed values of fracture toughness, in mode I and mode II, can be distinguished at 0° orientation. For the PPA GF33, the error bars intersect, meaning that an overlapping of values can be possible. For PPS GF40, the overlapping is more visible. For 90° orientation, the fracture toughness differs in mode I and mode II.

The plain strain deformation condition according to ASTM E399 was verified using:

$$a \text{ and } t \geq 2.5 \left(\frac{K_I}{f_u}\right)^2 \tag{3}$$

where $f_u$ is the tensile strength. All other quantities were previously defined. If we quantify the right part of the eq. (3), will arrive at values in between 3.9 mm and 19.3 mm. The crack length (a = 20 mm) and the ligament (h-a) fulfill this criterion. In all cases, the specimen thickness (t = 3.27 mm) does not meet this request. However, the thickness of the plates does not allow to use thicker specimens.

A scanning electron microscope (SEM) was used to better visualize the fracture area. These captures can be seen in Fig. 9 (b), function of orientation angle. In Fig. 9 (a), a graphic representation of the failure mechanism at the tip of the crack was drawn for the two extreme cases: 0° and 90° orientation. The fracture for the 0° orientation case occurs mostly in the matrix and not at the fiber level. The reason behind this is due to how the fibers are aligned as a result of the injection molding process.

The combination of fibers and polymer matrix leads to different failure mechanisms such as: fiber fracture, fiber pull-out, fiber/matrix debonding and matrix fracture. If we take a closer look at Fig. 9 (b) (SEM photos), we can distinguish these types of failures. For 0°, fiber/matrix debonding can be seen as a failure mechanism. Small number of fibers are fractured or pulled. Looking at the 90° orientation case, the SEM photo is quite different. The longitudinal fibers cannot be seen. A multitude of tiny black holes can be observed that represent the fiber pull-out failure mechanism combined with fiber fracture. For the 45°, a combination of the main mechanisms noticed for 0° and 90° is identified.

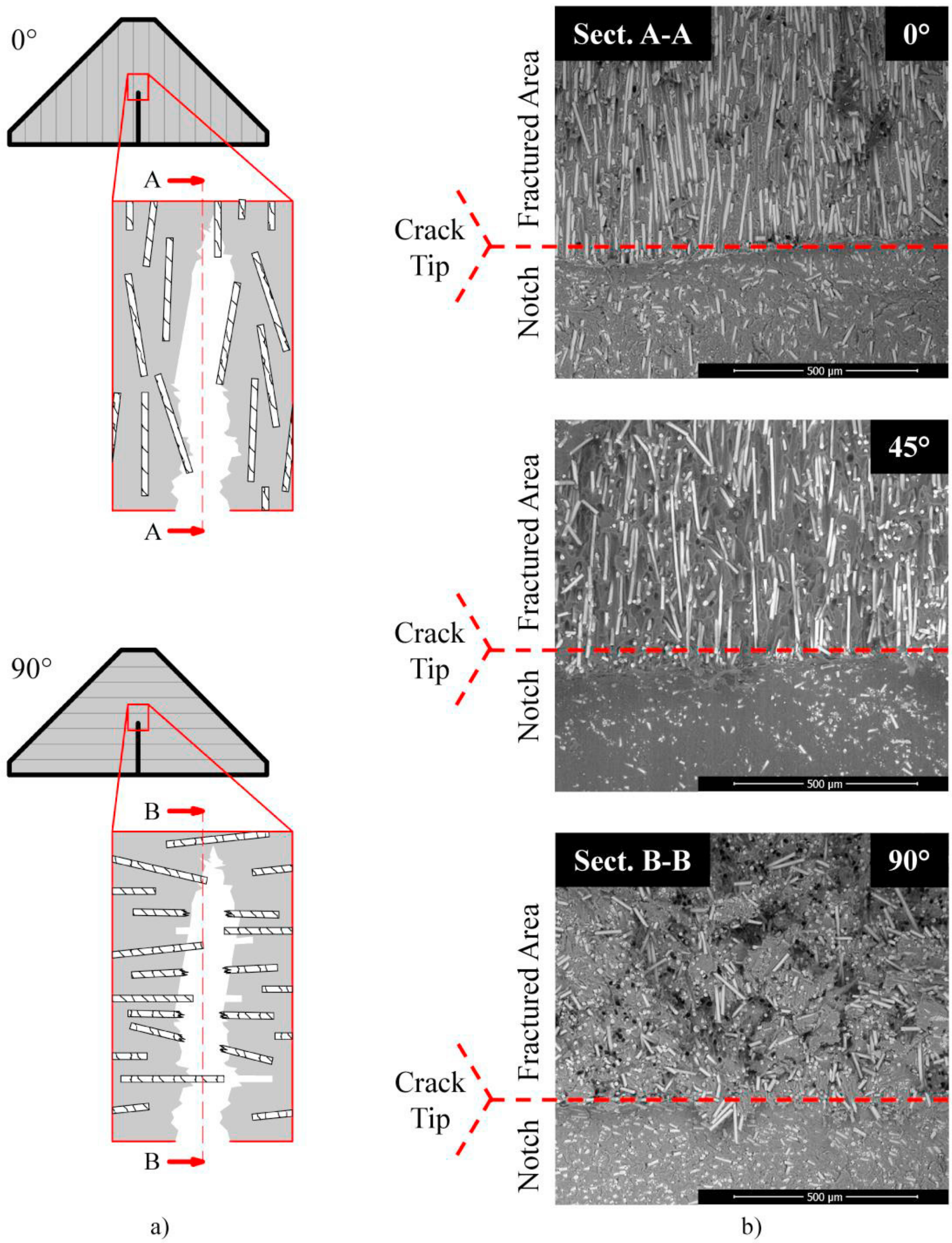


Fig. 9. Fracture schematics for 0° and 90° orientations (a) and SEM photos of the fractured area at different orientations (b).

## 5. Conclusions

The paper investigates the influence of the fiber orientation on fracture toughness of two polymeric materials reinforced with glass fibers. The ECT specimens were adopted and symmetrically loaded for mode I fracture toughness and asymmetrically loaded for mode II fracture toughness determination. The influence of the fiber orientation on fracture toughness was observed for both PPA and PPS materials.

The values of $K_{Ic}$ toughness for PPA are in the 6 to 10 MPa√m range, with a proportional increasing tendency of the toughness with fiber orientation. This phenomenon can be associated with 0° fiber orientation tensile strength tests, as both have fibers aligned to oppose the crack opening forces by creating a bridging effect between the sides of the crack.

For $K_{IIc}$ toughness in mode II, values are in the 4 to 6 MPa√m range, with a decreasing tendency of toughness as the fiber orientation increases. This fact could be explained by either fibers shearing at the crack tip or the crack propagating between the tips of the fibers, as in failure of the matrix material, phenomenon occurring easier due to the short length of the fibers.

For the PPS material, the $K_{Ic}$ and $K_{IIc}$ for mode I and respectively mode II have the same tendencies as for the PPA material. For mode I, the $K_{Ic}$ fracture toughness is rising from 5.5 MPa√m, for 0° orientation, to 8 MPa√m for 90° fiber orientation specimens. Similar values have been found by Friedrich 1985 and also by Karger-Kocsis and Friedrich 1987.

In failure mode II, the $K_{IIc}$ fracture toughness has a slightly decreasing tendency, from 5.5 MPa√m, at 0° orientation, to 5 MPa√m, at 90° fiber orientation. Fracture toughness values for PPA material have not been found in literature to compare with.

## Acknowledgements

The project leading of this application has received funding from the European Union's Horizon 2020 research and innovation program under grant agreement No 857124 and by a grant of the Ministry of Education and Research, CNCS/CCCDI - UEFISCDI, project number PN-III-P3-3.6-H2020-2020-0079/ contract No 27/2021.

## References

Aliha, M. R.M., A. Bahmani, and Sh Akhondi. 2016. "Mixed Mode Fracture Toughness Testing of PMMA with Different Three-Point Bend Type Specimens." European Journal of Mechanics, A/Solids 58: 148–62. http://dx.doi.org/10.1016/j.euromechsol.2016.01.012.

Aliha, M. R.M., Gh R. Hosseinpour, and M. R. Ayatollahi. 2013. "Application of Cracked Triangular Specimen Subjected to Three-Point Bending for Investigating Fracture Behavior of Rock Materials." Rock Mechanics and Rock Engineering 46(5): 1023–34.

Bernasconi, A., P. Davoli, A. Basile, and A. Filippi. 2007. "Effect of Fibre Orientation on the Fatigue Behaviour of a Short Glass Fibre Reinforced Polyamide-6." International Journal of Fatigue 29(2): 199–208.

Friedrich, K. 1985. "Microstructural Efficiency and Fracture Toughness of Short Fiber/Thermoplastic Matrix Composites." Composites Science and Technology 22(1): 43–74.

Holmström, Petter Henrik, Odd Sture Hopperstad, and Arild Holm Clausen. 2020. "Anisotropic Tensile Behaviour of Short Glass-Fibre Reinforced Polyamide-6." Composites Part C: Open Access 2: 100019.

Jørgensen, Jens Kjær, Erik Andreassen, and Dietmar Salaberger. 2019. "The Effect of Fiber Concentration on Fiber Orientation in Injection Molded Film Gated Rectangular Plates." Polymer Composites 40(2): 615–29.

Karger-Kocsis, J., and K. Friedrich. 1987. "Microstructural Details and the Effect of Testing Conditions on the Fracture Toughness of Injection-Moulded Poly (Phenylene-Sulphide) Composites." Journal of Materials Science 22(3): 947–61.

Karger-Kocsis, J, and K Friedrich. 1988. "Fracture Behavior of Injection-Molded Short and Long Glass Fiber-Polyamide 6.6 Composites." Composites Science and Technology 32(4): 293–325.

Köbler, Jonathan et al. 2018. "Fiber Orientation Interpolation for the Multiscale Analysis of Short Fiber Reinforced Composite Parts." Computational Mechanics 61(6): 729–50.

Micota, Dan, Alexandru Isaincu, and Liviu Marşavina. 2021. "Experimental Testing of Two Short-Fiber Reinforced Composites: PPA-GF33 and PPS-GF40." Material Design and Processing Communications 3(6): 2–8.

Tanaka, Keisuke, Takuya Kitano, and Noboru Egami. 2014. "Effect of Fiber Orientation on Fatigue Crack Propagation in Short-Fiber Reinforced Plastics." Engineering Fracture Mechanics 123: 44–58.

Torabi, Ehsan, Saeid Ghouli, Liviu Marșavina, and Majid R. Ayatollahi. 2021. "Mixed Mode Fracture Behavior of Short-Particle Engineered Wood." Theoretical and Applied Fracture Mechanics 115.

Wawrzynek, Paul, Ingraffea, Anthony, FRANC2D A Two Dimensional Crack Propagation Simulator, User Guide, Version 3.1, 1993, Cornell.